

# Growth, Microstructure and Electrochemical Properties of RF Sputtered $\text{LiMn}_2\text{O}_4$ Thin Films on Au/Polyimide Flexible Substrates

K. Jayanth Babu, P. Jeevan Kumar, Obili M. Hussain\*

Thin Film Laboratory, Department of Physics, Sri Venkateswara University, Tirupati, India.  
Email: [hussainsvu@gmail.com](mailto:hussainsvu@gmail.com)

Received October 26<sup>th</sup>, 2012; revised November 25<sup>th</sup>, 2012; accepted December 16<sup>th</sup>, 2012

## ABSTRACT

$\text{LiMn}_2\text{O}_4$  thin films are deposited on gold coated polyimide flexible substrates using RF magnetron sputtering technique maintained at a moderate substrate temperature of 300°C. The films exhibited characteristic peaks with predominant (111) orientation representing cubic spinel structure of  $Fd3m$  symmetry with an evaluated lattice parameter of 8.199 Å. The surface topography of films exhibited pyramidal shaped grains oriented vertical to the substrate surface with root mean square surface roughness of 90 nm. The Pt/ $\text{LiMn}_2\text{O}_4$  electrochemical cell in aqueous region exhibited two step de-insertion and insertion kinetics of Li ion during oxidation and reduction reaction with an initial discharge capacity of  $36 \mu\text{Ah}\cdot\text{cm}^{-2}\cdot\mu\text{m}^{-1}$ .

**Keywords:**  $\text{LiMn}_2\text{O}_4$  Thin Films; RF-Sputtering; Flexible Kapton Substrates; Microstructure

## 1. Introduction

In the existing prompt developing science and technology decade, much attention has been devoted to the development of all solid state thin film microbatteries to power the miniaturized micro and nano electronic devices such as MEMS and NEMS [1,2]. The realization of such microbatteries is originated from the synthesis and properties of thin film cathode materials with high energy density and specific capacity [3,4]. Lithium manganese oxide ( $\text{LiMn}_2\text{O}_4$ ) with spinel structure is one of the most extensively studied cathode material for  $\text{Li}/\text{Li}^+$  rechargeable batteries due to its low cost, non-toxicity and relatively high energy density [5-13]. Most of the researchers prepared  $\text{LiMn}_2\text{O}_4$  thin films on solid substrates using various physical [14-19] and chemical [20,21] vapour deposition techniques and studied their electrochemical performance and durability at device level [22]. But, the fabrication of thin film coatings on polyimide flexible substrate is a challenging and novel research area for the future cutting-edge technologies. Since, they are flexible, so that they can bent and stick to any curved shape objects without altering its basic properties, they are weightless and are easy to carry and can be folded. To the best of our knowledge, no reports are available explaining the growth, microstructure, and electrochemical properties of  $\text{LiMn}_2\text{O}_4$  thin films on

flexible polymer substrates using RF magnetron sputtering technique. Bing-Joe Hwang *et al.* [23] deposited  $\text{LiMn}_2\text{O}_4$  films on ITO coated Pt/Al flexible substrates using RF magnetron sputtering technique and observed a discharge capacity of 67.5 mAh/g. Hee-Soo Moon *et al.* [24] deposited  $\text{LiMn}_2\text{O}_4$  thin films on stainless steel substrates using RF magnetron sputtering and reported a discharge capacity of  $24 \mu\text{Ah}\cdot\text{cm}^{-2}\cdot\mu\text{m}^{-1}$ . A discharge capacity of  $43.5 \mu\text{Ah}\cdot\text{cm}^{-2}\cdot\mu\text{m}^{-1}$  was observed for ten cycles by Jayanth *et al.* [25] for the  $\text{LiMn}_2\text{O}_4$  films deposited on metallized silicon substrates using RF magnetron sputtering technique.

Among the various physical vapour deposition techniques, RF magnetron sputtering technique is observed to be one of the most favorable and industrially viable technique since it enables the formation of homogeneous films with definite thickness along with good adhesion. The chief advantage is that RF magnetron sputtering activates broad ionization even at low sputtering powers and allow the film to crystallize at moderate substrate temperatures, especially during long sputtering times. Also, the microstructural properties can be altered by properly controlling the deposition parameters. Hence, in the present investigation, thin films of  $\text{LiMn}_2\text{O}_4$  are deposited on Au/polyimide flexible substrates using RF magnetron sputtering technique at a moderate substrate temperature and studied the growth and microstructural properties. The electrochemical properties are studied in

\*Corresponding author.

aqueous electrolyte media by investigating cyclic voltammetry and chronopotentiometry measurements.

## 2. Experimental

LiMn<sub>2</sub>O<sub>4</sub> thin films are deposited from a three inch diameter cold pressed and sintered lithium rich (10%) LiMn<sub>2</sub>O<sub>4</sub> target using RF magnetron sputtering technique on gold coated polyimide (Kapton) substrates (obtained from M/s Aarthai engineers). During the depositions, the substrate temperature was kept at 300°C and the sputtered gas (O<sub>2</sub>/Ar) composition of 1:6 was maintained to minimize the loss of lithium [26]. The RF power applied to the LiMn<sub>2</sub>O<sub>4</sub> target during sputtering was 140 W. The sputtering pressure maintained during the deposition was 0.9 pascals. The thickness of the films was 0.8 μm. The structural properties were studied by the X-ray diffraction technique (Siefert computerized X-ray diffractometer, model 3003 TT). The surface morphological characteristics of the films have been studied by scanning electron microscope (Carl Zeiss, EVO MA 15). The electrochemical measurements like cyclic voltammetry (CV) and chronopotentiometry (CP) were performed by designing a prototype aqueous electrochemical cell to understand the fast transport kinetics of the Li-ions in LiMn<sub>2</sub>O<sub>4</sub> thin film positive electrode. The design of the cell (Pt/LiMn<sub>2</sub>O<sub>4</sub>) was comprises of three-electrodes which were electrochemically suffused in saturated Li<sub>2</sub>SO<sub>4</sub> aqueous electrolyte media (Pt/saturated Li<sub>2</sub>SO<sub>4</sub>/LiMn<sub>2</sub>O<sub>4</sub> film). The RF sputtered LiMn<sub>2</sub>O<sub>4</sub> thin film deposited on gold coated polyimide Kapton substrates was employed as working electrode (cathode). A platinum counter electrode (anode), which acts as a reversible source and sink of lithium (conducting) ions, and a commercial calomel reference (Hg/Hg<sup>+</sup>) electrode by which the electrochemical analysis was calibrated in the presence of saturated Li<sub>2</sub>SO<sub>4</sub> aqueous solution as electrolyte, were employed. CHI 608C (CH Instruments Inc., USA) electrochemical analyzer was used for the aqueous cell measurements and is operated in the cut-off voltage region 0.0 - 1.2 V.

## 2. Results and Discussion

### 2.1. Microstructural Properties

**Figure 1** shows the XRD pattern of LiMn<sub>2</sub>O<sub>4</sub> films deposited on Au/polyimide substrates maintained at 300°C. All the diffraction peaks are ascribed to the spinel structure of LiMn<sub>2</sub>O<sub>4</sub>. The films exhibited characteristic peaks with predominant (111) orientation representing cubic spinel structure of Fd3m symmetry, in which the oxygen ions are placed on a face-centered cubic array. The lithium ions occupy the tetrahedral 8a sites of the oxide network, whereas the Mn is placed in the octahedral 16c

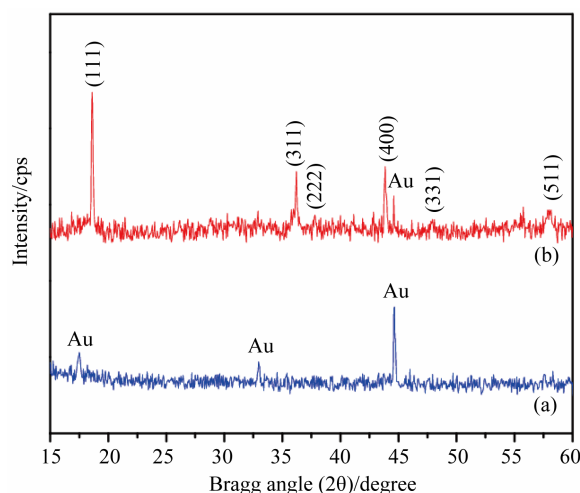


**Figure 1.** The X-ray diffraction patterns of (a) Au/Kapton substrate and (b) LiMn<sub>2</sub>O<sub>4</sub> thinfilms on Au/Kapton substrates.

sites [17]. The lattice parameter, and Mn-O interatomic distances were also calculated for the films by considering full width at half maximum (FWHM) value of (111) orientation and oxygen positional parameter (u) as 0.265 [25] and are observed to be 8.199 Å, 2.898 Å and 1.918 Å respectively. The lattice parameter of bulk LiMn<sub>2</sub>O<sub>4</sub> at room temperature was 8.246 Å [27]. The lower value of lattice parameter is due to the presence of compressional strain in the films [28]. The micro-strain within the crystallite ( $\epsilon$ ) was estimated considering the full width half maxima (FWHM) of predominant (111) orientation using the formula proposed by Li and coworkers [29]:

$$\epsilon = (\beta_{1/2} \cot \theta) / 4 \quad (1)$$

The corresponding strain observed for the films deposited at a moderate substrate temperature of 573 K was  $4.5 \times 10^{-3}$ . From XRD studies the average grain size for the films was calculated by considering FWHM values and is observed to be as 190 nm.

The Raman scattering measurements were carried out for the LiMn<sub>2</sub>O<sub>4</sub> film deposited on Au/Flexible substrates and the spectrum is shown in **Figure 2**. The Raman spectrum revealed all vibrational peaks resembled as developed in solid substrates [30]. As per the factor group analysis for the Fd3m symmetry five Raman modes ( $A_{1g} + E_g + 3F_{2g}$ ) at 366, 427, 484, 581, 625 cm<sup>-1</sup> are located at their respective positions. The main band at 625 cm<sup>-1</sup> has  $A_{1g}$  symmetry and corresponds to the symmetric Mn-O stretching vibration of MnO<sub>6</sub> groups. The bands at 427 and 484 cm<sup>-1</sup> can be assigned to Li-O vibrations of LiO<sub>4</sub> groups. The band at 366 cm<sup>-1</sup> may correspond to the bending vibration of MnO<sub>6</sub> groups. These results indicate that LiMn<sub>2</sub>O<sub>4</sub> films deposited on flexible Kapton substrates have cubic spinel structure.

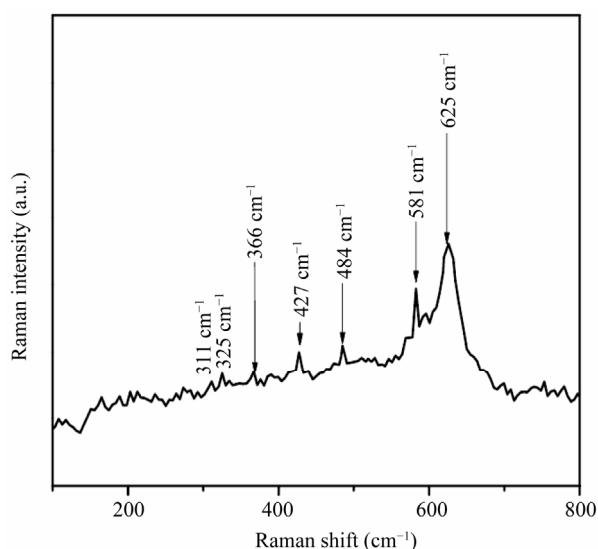


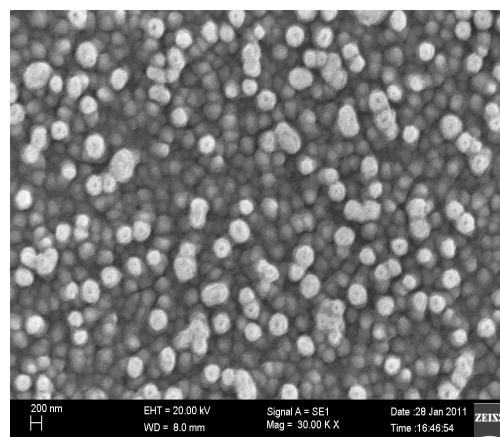
**Figure 2.** The Raman spectra of the film deposited on flexible substrates.

## 2.2. Surface Morphological Studies

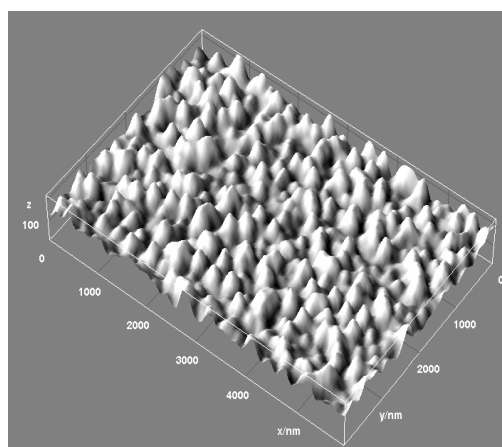
The scanning electron micrograph of  $\text{LiMn}_2\text{O}_4$  thin films is shown in **Figure 3(a)**. The morphological growth of  $\text{LiMn}_2\text{O}_4$  films is observed to be improved by the nucleation of large size target particulates with high rate of deposition incepted by increasing the RF power *i.e.* at 140 W and is shown in **Figure 3(a)**. The 3D surface texture of the SEM image was subjected to image processing using “imageJ” software (model 1.44p) and is shown in **Figure 3(b)**.

The image processing of the SEM images were carried out in two steps: 1) denoising using a median filter of radius 9.3 nm (2 pixels); 2) Quantification of grain surface area fraction and surface roughness using the “3D” and “roughness calculation” Java pug-ins [31]. The surface of the films is composed of vertically aligned nanocrystalline columns which are uniformly distributed. The growth of grains are observed to be perpendicular to the substrate surface which leads to the existence of more stress and strain components in the deposited films which has lower lattice parameter in films as observed from XRD data. The surface cross section of  $\text{LiMn}_2\text{O}_4$  columns is observed to have a roughness of about 90 nm (obtained from imageJ software) provided with sharp headed nano grains of average grain size of the order of 164 nm.

The surface nucleation and film formation density on flexible polymer is quite critical because of poor rate of adatom mobility induced by the lower aggregation energy of the sputter ejected particles on the substrate surface [32]. Since the kinetic energy of the incident positive ions is proportional to the applied power. To im-



(a)



(b)

**Figure 3.** (a) The SEM image of  $\text{LiMn}_2\text{O}_4$  thin films; (b) The 3D surface topography of  $\text{LiMn}_2\text{O}_4$  thin films.

prove the sputtering yield the RF power was maintained at 140 W where the observed deposition rate was 150  $\text{\AA}/\text{min}$ . The ejected large particle from the target at this power processes to have higher kinetic energy and impinges onto the substrate surface and initiates the growth. At constant substrate temperature, the adatom mobility is constant on the surface of the substrate and favors the formation of greater number of crystallite centers rather than the coalescence of islands. The enhancement of crystallite size and the surface roughness of the films grown on flexible substrate is a positive observation for electrochemical research. Generally this type of surface topographical features of  $\text{LiMn}_2\text{O}_4$  films is more favorable for obtaining improved electrochemical response of positive electrode films.

## 2.3. Electrochemical Studies

**Figure 4** shows the cyclic voltammogram recorded at a scan rate of  $0.5 \text{ m}\cdot\text{Vs}^{-1}$  for  $\text{LiMn}_2\text{O}_4$  thin film deposited on Au coated polyimide flexible Kapton substrate. Two

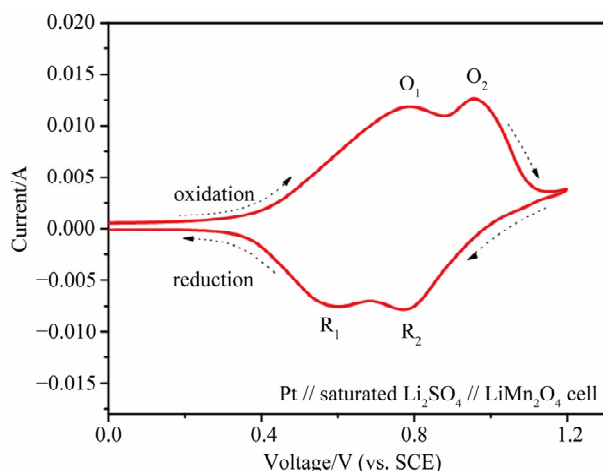


**Figure 4.** The cyclic voltammogram of  $\text{LiMn}_2\text{O}_4$  thin film at a sweep rate of  $0.5 \text{ m}\cdot\text{Vs}^{-1}$ .

sets of well-separated peaks are clearly seen, which correspond to the potential plateaus. The peaks located at 0.789 V and 0.961 V during cathodic scan corresponding to the Li ion deintercalation from  $\text{LiMn}_2\text{O}_4$  host matrix to form  $\lambda\text{-MnO}_2$ , while the peaks located at 0.590 V and 0.773 V during anodic scan correspond to Li ion intercalation in to  $\lambda\text{-MnO}_2$  to form  $\text{LiMn}_2\text{O}_4$ . This two step deinserted and inserted kinetics of Li ion during oxidation and reduction reactions indicates characteristic property of the spinel  $\text{LiMn}_2\text{O}_4$  [33]. In the spinel  $\text{LiMn}_2\text{O}_4$ , lithium ions occupy tetrahedral (8a) sites, Mn ions occupy ( $\text{Mn}^{3+}/\text{Mn}^{4+}$ ) octahedral (16d) sites and  $\text{O}^{2-}$  ions occupy (32e) sites. The oxygen ions form a cubic close-packed array, tetrahedral (8a) sites share face with vacant octahedral sites (16c), so that they form a three dimensional vacant channels. Lithium ions can intercalate/de-intercalate through these channels during the electrochemical reaction [34].

The first oxidation peak ( $\text{O}_1$ ) at 0.789 V is attributed to the removal of lithium ions from half of the tetrahedral sites, whereas the second oxidation peak ( $\text{O}_2$ ) at 0.961 V is due to the removal of lithium ions from the remaining tetrahedral sites. **Figure 5** shows the first discharge curve of  $\text{LiMn}_2\text{O}_4$  thin film. It can be seen that the discharge curve for the film have two distinct potential plateaus, which is in agreement with the reduction potentials observed from the cyclic voltammogram. The upper plateau region of the discharge curve represents a two-phase equilibrium between  $\lambda\text{-MnO}_2$  and  $\text{Li}_{0.5}\text{Mn}_2\text{O}_4$ , whereas the second plateau represents phase equilibrium between  $\text{Li}_{0.5}\text{Mn}_2\text{O}_4$  and  $\text{LiMn}_2\text{O}_4$ . The discharge capacity for the films is estimated to be around  $36 \mu\text{Ah}\cdot\text{cm}^{-2}\cdot\mu\text{m}^{-1}$  for the first cycle. The low discharge capacity may be due to presence of small grains and high compressional stresses in the films. The discharge capacity for ten cycles is shown in **Figure 6**. The discharge capacity was decrea-

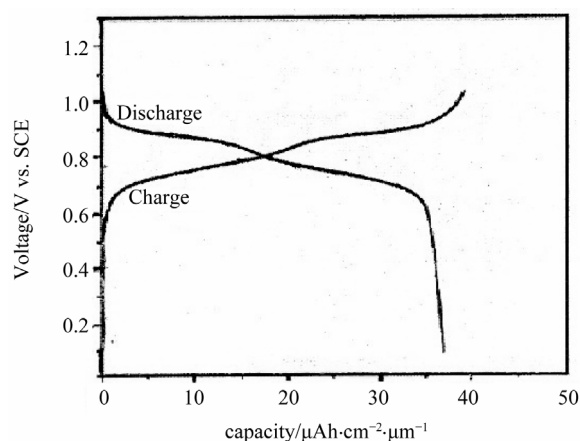


**Figure 5.** The first charge-discharge curve of flexible  $\text{LiMn}_2\text{O}_4$  thin film.

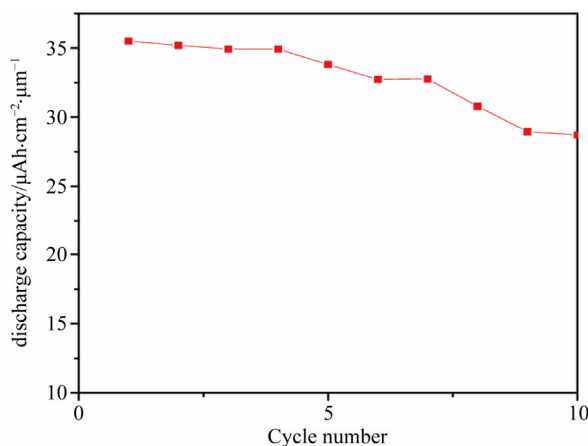


**Figure 6.** The discharge capacity of  $\text{LiMn}_2\text{O}_4$  thin film for ten cycles.

sed to  $32.8 \text{ mAh}/\text{cm}^2 \cdot \text{mm}$  for 10 cycles. The platinum counter electrode couldn't act as a perfect reversible source and sink of lithium ions and may be one of the reason for the low cyclic retention of the Pt/ $\text{LiMn}_2\text{O}_4$  cells. However the results are seem to be encouraging and further investigations are in progress to understand detailed electrochemical behavior of the films.

### 3. Conclusion

$\text{LiMn}_2\text{O}_4$  films are deposited successfully on metallized polyimide flexible substrates at a moderate temperature of  $300^\circ\text{C}$  using RF magnetron sputtering technique. The films exhibited predominant (111) orientation along with the characteristic peaks representing cubic spinel structure with Fd3m symmetry. The calculated lattice parameter, Mn-Mn and Mn-O interatomic distances are observed to be 8.199 Å, 2.898 Å and 1.918 Å respectively. From "imageJ" analysis of SEM data the root mean square roughness (RMS) are observed to be 90 nm with

an average grain size of 164 nm. From slow scan cyclic voltammetry (SSCV) studies, the presence of two well separated electrochemically active redox peaks during oxidation and reduction reactions indicate the characteristic property of the spinel  $\text{LiMn}_2\text{O}_4$  structure in the films. The Pt/ $\text{LiMn}_2\text{O}_4$  electrochemical cell with  $\text{LiMn}_2\text{O}_4$  film coated on metallized flexible Kapton substrates exhibited an initial discharge capacity of about  $36 \mu\text{Ah}\cdot\text{cm}^{-2}\cdot\mu\text{m}^{-1}$  for the first cycle which is an encouraging result. Further investigations are in progress to improve the electrochemical properties such as capacity and cycling life.

#### 4. Acknowledgements

This research work is supported by DRDO and one of the authors Mr. Jayanth is highly thankful to DST for providing necessary financial assistance to carry out this work under Promotion of University Research and Scientific Excellence (PURSE) programme.

#### REFERENCES

- [1] K.-L. Lee, J.-Y. Jung, S.-W. Lee, H.-S. Moon and J.-W. Park, "Electrochemical Characteristics and Cycle Performance of  $\text{LiMn}_2\text{O}_4/\text{a-si}$  Microbattery," *Journal of Power Sources*, Vol. 130, No. 1-2, 2004, pp. 241-246. [doi:10.1016/j.jpowsour.2003.11.059](https://doi.org/10.1016/j.jpowsour.2003.11.059)
- [2] W. W. Sun, F. Cao, Y. M. Liu, X. Z. Zhao, X. G. Liu and J. K. Yuan, "Nonporous  $\text{LiMn}_2\text{O}_4$  Nanosheets with Exposed (111) Facets as Cathodes for Highly Reversible Lithium-Ion Batteries," *Journal of Materials Chemistry*, Vol. 22, 2012, pp. 20952-20957. [doi:10.1039/c2jm32658b](https://doi.org/10.1039/c2jm32658b)
- [3] C. Y. Sun, H. Y. Yang, J. Xie, G. S. Cao, X. B. Zhao and T. J. Zhu, "Nanoparticles-Assembly of  $\text{LiMn}_2\text{O}_4$  Hollow Microspheres with Improved Rate Capability and Cycleability for Lithium Ion Batteries," *International Journal of Electrochemical Science*, Vol. 7, No. 7, 2012, pp. 6191-6201.
- [4] Y. Kim, J. Lim and S. Kang, "Investigation on the Dissolution of Mn Ions from  $\text{LiMn}_2\text{O}_4$  Cathode in the Application of Lithium Ion Batteries: First Principle Molecular Orbital Method," *International Journal of Quantum Chemistry*, Vol. 113, No. 2, 2012, pp. 148-154. [doi:10.1002/qua.24314](https://doi.org/10.1002/qua.24314)
- [5] S. Komaba, N. Kumugai, M. Baba, F. Miura, N. Fujita, H. Groult, D. Devilliers and B. Kaplan, "Preparation of Li-Mn-O Thinfilms by r.f-Sputtering Method and Its Application to Rechargeable Batteries," *Journal of Applied Electrochemistry*, Vol. 30, No. 10, 2000, pp. 1179-1182. [doi:10.1023/A:1004047614084](https://doi.org/10.1023/A:1004047614084)
- [6] C. C. Chen, K. F. Chiu, K. M. Lin, H. C. Lin, C.-R. Yang and F. M. Wang, "Combinational Effects of Oxygen Plasma Irradiation and Annealing on  $\text{LiMn}_2\text{O}_4$  Thinfilm Cathodes," *Journal of Electrochemical Science*, Vol. 158, No. 3, 2011, pp. A262-A265. [doi:10.1149/1.3531988](https://doi.org/10.1149/1.3531988)
- [7] A. S. Arico, P. Bruce, B. Scrosati, J. M. Tarascon and W. van Schalkwijk, "Nanostructured Materials for Advanced Energy Conversion and Storage Devices," *Nature Materials*, Vol. 4, 2005, pp. 366-367. [doi:10.1038/nmat1368](https://doi.org/10.1038/nmat1368)
- [8] S. Y. Chung, J. T. Bloking and Y. M. Chiang, "Electronically Conductive Phospho-Olivines as Lithium Storage Electrodes," *Nature Materials*, Vol. 1, 2002, pp. 123-128. [doi:10.1038/nmat732](https://doi.org/10.1038/nmat732)
- [9] P. L. Taberna, S. Mitra, P. Poizot, P. Simon and J. M. Tarascon, "High Rate Capabilities  $\text{Fe}_3\text{O}_4$ -Based Cu Nano Architected Electrodes for Lithium-Ion Battery Applications," *Nature Materials*, Vol. 5, 2006, pp. 567-573. [doi:10.1038/nmat1672](https://doi.org/10.1038/nmat1672)
- [10] H. Li, Z. Wang, L. Chen and X. Huang, "Research on Advanced Materials for Li-Ion Batteries," *Advanced Materials*, Vol. 21, No. 45, 2009, pp. 4593-4607. [doi:10.1002/adma.200901710](https://doi.org/10.1002/adma.200901710)
- [11] P. Bruce, B. Scrosati and J. M. Tarascon, "Nanomaterials for Rechargeable Lithium Batteries," *Angewandte Chemie International Edition*, Vol. 47, No. 16, 2008, pp. 2930-2946. [doi:10.1002/anie.200702505](https://doi.org/10.1002/anie.200702505)
- [12] Z. Yang, J. Zhang, M. C. W. Kintner-Meyer, X. Lu, D. Choi, J. P. Lemmon and J. Liu, "Electrochemical Energy Storage for Green Grid," *Chemical Reviews*, Vol. 111, No. 5, 2011, pp. 3577-3614. [doi:10.1021/cr100290v](https://doi.org/10.1021/cr100290v)
- [13] L. Ji, Z. Lin, M. Alcoutlabi and X. Zhang, "Recent Developments in Nanostructured Anode Materials for Rechargeable Lithium-Ion Batteries," *Energy & Environmental Science*, Vol. 4, No. 8, 2011, pp. 2682-2699. [doi:10.1039/c0ee00699h](https://doi.org/10.1039/c0ee00699h)
- [14] K. A. Striebel, C. Z. Deng, S. J. Wen and E. J. Cairns, "Electrochemical Behavior of  $\text{LiMn}_2\text{O}_4$  and  $\text{LiCoO}_2$  Thinfilms Produced with Pulsed Laser Deposition," *Journal of the Electrochemical Society*, Vol. 143, No. 6, 1996, pp. 1821-1827. [doi:10.1149/1.1836910](https://doi.org/10.1149/1.1836910)
- [15] O. M. Hussain, K. Harikrishna, V. Kalaivani and C. M. Julien, "Structural and Electrical Properties of Lithium Manganese Oxide Thin Films Grown by Pulsed Laser Deposition," *Ionics*, Vol. 13, No. 6, 2007, pp. 455-459. [doi:10.1007/s11581-007-0134-7](https://doi.org/10.1007/s11581-007-0134-7)
- [16] V. Kalai Vani and O. M. Hussain, "Synthesis and Characterization of Electron Beam Evaporated  $\text{LiCoO}_2$  Thin Films," *Ionics*, Vol. 13, No. 6, 2007, pp. 473-477. [doi:10.1007/s11581-007-0141-8](https://doi.org/10.1007/s11581-007-0141-8)
- [17] F. Y. Shih and K. Z. Fung, "Effect of Annealing Temperature on Electrochemical Performance of Thinfilm  $\text{LiMn}_2\text{O}_4$  Cathode," *Journal of Power Sources*, Vol. 153, 2006, pp. A179-A185.
- [18] N. J. Dudney, J. B. Bates, R. A. Zuhr, S. Young, J. D. Robertson, H. P. Jun and S. A. Hackney, "Nanocrystalline  $\text{Li}_x\text{Mn}_{2-y}\text{O}_4$  Cathodes for Solid-State Thin-Film Rechargeable Lithium Batteries," *Journal of the Electrochemical Society*, Vol. 146, No. 7, 1999, pp. 2455-2464. [doi:10.1149/1.1391955](https://doi.org/10.1149/1.1391955)
- [19] K. H. Hwang, S. H. Lee and S. K. Joo, "Characterization of Sputter-Deposited  $\text{LiMn}_2\text{O}_4$  Thinfilms for Rechargeable Microbatteries," *Journal of the Electrochemical Society*, Vol. 141, No. 12, 1994, pp. 3296-3299. [doi:10.1149/1.2059329](https://doi.org/10.1149/1.2059329)

- [20] P. Liu, J. G. Zhang, J. A. Turner, C. E. Tracy and D. K. Benson, "Lithium Manganese Oxide Thin Film Cathodes Prepared by Plasma Enhanced Chemical Vapor Deposition," *Journal of the Electrochemical Society*, Vol. 146 No. 6, 1999, pp. 2001-2005. [doi:10.1149/1.1391881](https://doi.org/10.1149/1.1391881)
- [21] W. Liu and X. Huang, "Studies of Stannic Oxide as an Anode Material for Lithium-Ion Batteries," *Journal of the Electrochemical Society*, Vol. 145, No. 1, 1998, pp. 59-62. [doi:10.1149/1.1838211](https://doi.org/10.1149/1.1838211)
- [22] J. F. M. Oudenhoven, L. Bagetto and P. H. L. Notten, "All-Solid State Lithium-Ion Microbatteries: A Reviews of Various Three-Dimensional Concepts," *Advanced Energy Materials*, Vol. 1, No. 1, 2011, pp. 10-33. [doi:10.1002/aenm.201000002](https://doi.org/10.1002/aenm.201000002)
- [23] B.-J. Hwang, C.-Y. Wang, M.-Y. Cheng and R. Santhanam, "Structure, Morphology, and Electrochemical Investigation of  $\text{LiMn}_2\text{O}_4$  Thin Film Cathodes Deposited by Radio Frequency Sputtering for Lithium Microbatteries," *The Journal of Physical Chemistry C*, Vol. 113, No. 26, 2009, pp. 11373-11380. [doi:10.1021/jp810881d](https://doi.org/10.1021/jp810881d)
- [24] H.-S. Moon and J.-W. Park, "Characteristics of In-Situ Annealed  $\text{LiMn}_2\text{O}_4$  Thinfilms for a MEMs Power System," *Journal of the Korean Physical Society*, Vol. 41, 2002, pp. 872-875.
- [25] K. J. Babu, P. J. Kumar and O. M. Hussain, "Microstructural and Electrochemical Properties of RF-Sputtered  $\text{LiMn}_2\text{O}_4$  Thin Film Cathodes," *Applied Nano Science*, Vol. 2, No. 4, 2012, pp. 401-407. [doi:10.1007/s13204-011-0054-8](https://doi.org/10.1007/s13204-011-0054-8)
- [26] K. J. Babu, P. J. Kumar, O. M. Hussain and C. M. Julien, "Influence of Annealing Temperature on Microstructural and Electrochemical Properties of Rf-Sputtered  $\text{LiMn}_2\text{O}_4$  Film Cathodes," *Journal of Solid State Electrochemistry*, Vol. 16, No. 10, 2012, pp. 3383-3390. [doi:10.1007/s10008-012-1784-6](https://doi.org/10.1007/s10008-012-1784-6)
- [27] F. Shinshu, S. Kaida, M. Nagayama and Y. Nitta, "X-Ray Absorption Fine Structure Study on Li-Mn-O Compounds:  $\text{LiMn}_2\text{O}_4$ ,  $\text{Li}_4\text{Mn}_5\text{O}_{12}$  and  $\text{LiMnO}_3$ ," *Journal of Power Sources*, Vol. 68, No. 2, 1997, pp. 609-612. [doi:10.1016/S0378-7753\(96\)02591-8](https://doi.org/10.1016/S0378-7753(96)02591-8)
- [28] S. Chitra, P. Kalyani and T. Mohan, "Characterization and Electrochemical Studies of  $\text{LiMn}_2\text{O}_4$  Cathode Materials Prepared by Combustion Method," *Journal of Electroceramics*, Vol. 3, No. 4, 1999, pp. 433-441. [doi:10.1023/A:1009982301437](https://doi.org/10.1023/A:1009982301437)
- [29] J. Li, J. Zhang, X. Zhang, C. Yang, N. Xu and B. Xia, "Study of the Storage Performance of a Li-Ion Cell at Elevated Temperature," *Electrochimica Acta*, Vol. 55, No. 3, 2010, pp. 927-934. [doi:10.1016/j.electacta.2009.09.077](https://doi.org/10.1016/j.electacta.2009.09.077)
- [30] C. Julien, E. Haro-Poniatowski, M. A. Camacho-Lopez, L. Escobar-Alarcon and J. Jimenez-Jarquín, "Growth of  $\text{LiMn}_2\text{O}_4$  Thinfilms Prepared by Pulsed-Laser Deposition and Their Electrochemical Properties in Lithium Microbatteries," *Materials Science and Engineering B*, Vol. 72, No. 1, 2000, pp. 36-72. [doi:10.1016/S0921-5107\(99\)00598-X](https://doi.org/10.1016/S0921-5107(99)00598-X)
- [31] F. Simmen, T. Lippert, P. Novák, B. Neuenchwander, M. Döbeli, M. Mallepell and A. Wokaun, "The Influence of Lithium Excess in the Target on the Properties and Compositions of  $\text{Li}_{1+x}\text{Mn}_2\text{O}_4$  Thinfilms Prepared by PLD," *Applied Physics A*, Vol. 93, No. 3, 2008, pp. 711-716. [doi:10.1007/s00339-008-4701-1](https://doi.org/10.1007/s00339-008-4701-1)
- [32] P. J. Kumar, K. J. Babu and O. M. Hussain, "RF Magnetron Sputter Deposited Nanocrystalline  $\text{LiCoO}_2$  Film Cathodes on Flexible Substrates," *Advanced Science, Engineering and Medicine*, Vol. 4, No. 3, 2012, pp. 190-199. [doi:10.1166/asem.2012.1147](https://doi.org/10.1166/asem.2012.1147)
- [33] W. Li and J. R. Dahn, "Lithium Ion Cells with Aqueous Electrolytes," *Journal of the Electrochemical Society*, Vol. 142, No. 6, 1995, pp. 1742-1746. [doi:10.1149/1.2044187](https://doi.org/10.1149/1.2044187)
- [34] M. Okubo, Y. Mizuno, H. Yamada, J. Kim, E. Hosono, H. Zhou, T. Kudo and I. Honma, "Fast Li-Ion Insertion into Nanosized  $\text{LiMn}_2\text{O}_4$  without Domain Boundaries," *ACS Nano*, Vol. 4, No. 2, 2010, pp. 741-752. [doi:10.1021/mn9012065](https://doi.org/10.1021/mn9012065)